International Journal of Low-Carbon Technologies Advance Access published February 5, 2014

Investigation of concentrating and nonconcentrating evacuated tube solar water heaters using 2D particle imaging velocimetry

David A.G. Redpath*, Philip Dalzell, Philip W. Griffiths and Neil J. Hewitt
Centre for Sustainable Technologies, University of Ulster at Jordanstown, Newtownabbey, Co. Antrim BT38 9QB, UK

Abstract

Under transient climatic conditions, solar water heaters using heat pipes are more effective at capturing incident solar radiation than other equivalent sized solar water heaters. The cost must be reduced to improve uptake of such systems. To investigate two methods were considered by this study: thermosyphon fluid flow and reflective concentrators. A physical reconfigurable laboratory model of the manifold and associated condensers of a heat-pipe-evacuated tube system were fabricated; fluid circulation was via thermosyphonic action, particle imaging velocimetry derived velocity maps and the use of concentrators was simulated. When condenser spacing was doubled, the Nusselt number increased by 43%, the velocity by 55% but the heat transfer efficiency of the model manifold decreased by 9%. Potential annual energy savings of 10 207 GWh could be realized if such systems could be successfully fabricated.

Keywords: thermosyphon; fluid flow visualization; solar energy; particle imaging velocimetry; compound parabolic concentrators; evacuated tube solar water heaters

*Corresponding author.
d.redpath@ulster.ac.uk

Received 7 June 2013; revised 31 December 2013; accepted 4 January 2014

1 INTRODUCTION

Current typical installation costs of solar water heating systems in the UK, a northern maritime climate are ~£4800, with annual cost savings from a UK-based field trial reported as £60–85 [1]. The most recent set of statistics available on the UK market size for solar thermal collectors in terms of capacity (kW_{th}) and area [2] reported that, in 2012, the total area of glazed collectors in operation was 709 673 m^2 with a capacity of 459 899 $mkWh_{th}$. The total area and thermal capacity of flat plate and vacuum tube collectors installed in 2012 were 47 893 and 11 382 m^2 and 33 525 and 7967 kW_{th}, respectively. In northern maritime climates, evacuated tube solar water heaters (ETSWHs) utilizing heat-pipe absorbers for removal of solar gain are the most effective means of collecting solar energy [3–5] due to the unique thermophysical properties of heat pipes. Unfortunately, heat-pipe ETSWHs have higher capital costs than direct flow systems reducing their attractiveness to consumers. This research investigates the integration of two potential cost reduction methods; thermosyphon fluid circulation and reflective concentrators. By designing and commercializing such a system, a decrease in capital cost and reduced payback periods could be achieved. This would potentially increase the uptake of such solar water heating systems by stimulating consumer demands, reduce fossil fuel-based combustion for production of thermal energy and lower CO_2 emissions.

Previous research has reported that the efficiency of a solar water heater using thermosyphon fluid circulation (natural convective heat transfer) instead of forced convective heat transfer which requires a pump with an integrated control unit to transfer solar gain from the absorber to the hot water storage tank has a similar system efficiency [6]. Reflective concentrators' particularly compound parabolic concentrators (CPCs) [7] improve the efficiency of solar energy systems at higher temperatures as the area of 'hot' absorber is reduced, decreasing radiative heat losses producing thermal energy at more useful (higher) temperatures. Secondly, as the area of absorber is reduced, the cost of the system is reduced as the number of vacuum tubes required decreases [6].

Low-concentration ($1.1\times-2\times$) CPC systems could capture a substantial fraction of diffuse radiation [8] so could be potentially deployed in northern maritime climates to reduce cost and improve performance.

Globally, over 90% of installed domestic solar water heaters use thermosyphon fluid circulation to transfer solar gain from

International Journal of Low-Carbon Technologies 2014, 0, 1–5

doi:10.1093/ijlct/ctu004

the solar collector to the hot water storage tank [9]. Research on thermosyphon circulation for evacuated solar thermal systems has been mostly on direct flow systems subjected to climatic conditions that vary significantly from northern maritime regions. The thermal performance of a commercial close-coupled thermosyphon glass concentric counter flow ETSWH was evaluated using an internationally recognized test procedure [10]. Under the load conditions specified in the Australian solar water heating standards, this system achieved a 55% reduction in energy usage, when supplying thermal energy to preheat a domestic hot water supply [11]. A similar study [12] evaluated another commercial close-coupled thermosyphon glass concentric counter flow ETSWH using the same internationally recognized procedure. The experimental data were used to numerical model the collector, predicting thermal performance for this system as a solar preheater delivering nocturnal hot water loads for locations in Australia, China and Europe, to an accuracy of $\pm 5\%$. The experimental performance of water in glass ETSWH was measured by determining its optical and heat loss characteristics. Under the climatic conditions of Sydney, Australia, its efficiency was found to be lower than a similar sized flat-plate solar water heater [13] for delivery of domestic hot water.

Previous research on thermosyphon fluid circulation in different fluids such as air has been carried out. Experimentation by [14] generated interferograms of natural convective heat transfer fluid flows generated from heated vertical and inclined arrays of pin-fins. Other related studies on interactive pin-fin arrays and cylinders subject to natural convective heat transfer [12, 15–19] only considered idealized situations with regular but simple cavity geometries none of which were loop thermosyphons. The manifold chamber of the proprietary heat-pipe ETSWH under investigation in this article differs from the idealized situations considered by previous research by having an irregular six-sided cross section.

Thermosyphon fluid flow rates were measured to within $\pm 2\%$ using laser Doppler anemometry [20]. Images and velocity of natural convective fluid flows generated from physical laboratory all glass evacuated tube models were visualized using 2D-particle imaging velocimetry (2D-PIV) and compared with numerical simulations the results varied by $\pm 1.6\%$ The velocity of the thermosyphon fluid flow rate was sufficient to degrade thermal stratification within the hot water storage tank [19].

Some prior research investigating the performance of heat-pipe ETSWHs was undertaken at the University of Ulster's solar test facilities and indoor particle imaging velocimetry suite [21–23]. The performance of a physical laboratory model manifold was found comparable with that of an ETSWH when exposed to similar operating conditions; further details are provided in [21]. This article provides further data experimental work undertaken, investigating heat transfer within the manifold of thermosyphon heat-pipe ETSWHs discussing the significance and impact of the collected data. This work demonstrates that the thermofluidic phenomena that occur within the manifold of these systems simulated using a simplified physical model can be used for design improvements to be made using low-cost experiments. The significance of the results obtained, techniques derived from the experimental data for optimizing designs of thermosyphon ETSWHs are discussed and cost and energy reduction estimates for the UK solar thermal market are presented.

2 METHODOLOGY

The fabrication of the physical laboratory model, the setup of the PIV equipment and the experimental technique used to investigate the thermosyphon fluid flow regime are described in Sections 2.1–2.3, respectively.

2.1 Fabrication of Physical Laboratory Model Manifold

A physical laboratory model manifold constructed to the same dimensions as a 1-m^2 collector array was assembled at the University of Ulster. Its external and internal dimensions (mm) are shown in Figure 1.

The condenser array was physically simulated using solid copper cylinders (*pin-fins*) with an electric element (cartridge heater) inserted allowing the power supplied to be carefully controlled, maintained and higher heat fluxes on the condensers to be simulated.

2.2 Setup of 2D-PIV

PIV has the advantage of allowing the visualization of the instantaneous thermosyphon fluid flow field over an extended area using a single measurement [19]. To observe the displacement of fluid elements, the fluid flow under investigation was 'seeded' with small (20 μm) neutrally buoyant polyamide tracer particles, allowing these to travel at the same velocity as the fluid under investigation. A 2D-PIV analysis of the model manifold provided a visual interpretation of the interactions between the heat transfer fluid, pin-fins and enclosure walls. Image pairs were taken with a camera synchronized to the laser. Image processing software enabled tracking of particles through the flow field, allowing the magnitude and direction of the thermosyphon fluid flow to be quantified. The frequency of the laser pulses was set at 10 Hz with a camera exposure time of 10 000 μs.

2.3 Experimental Technique

From Figure 1 for the 10 pin-fin configuration, the first pin-fin, *pin-fin 1*, was on the left side beneath the inlet port and *pin-fin 10* beneath the outlet port. For the five pin-fin configuration, the pin-fin directly beneath the inlet port was removed and the pin-fin immediately to the right denoted as *pin-fin 1* the pin-fin beneath the outlet port was denoted as *pin-fin 5*. The design allowed the cartridge heaters to be replaced and pin-fins to be removed simulating the removal of evacuated tubes.

Under steady-state conditions at solar noon, the rate of heat transfer (Q) from each pin-fin/condenser to the surrounding

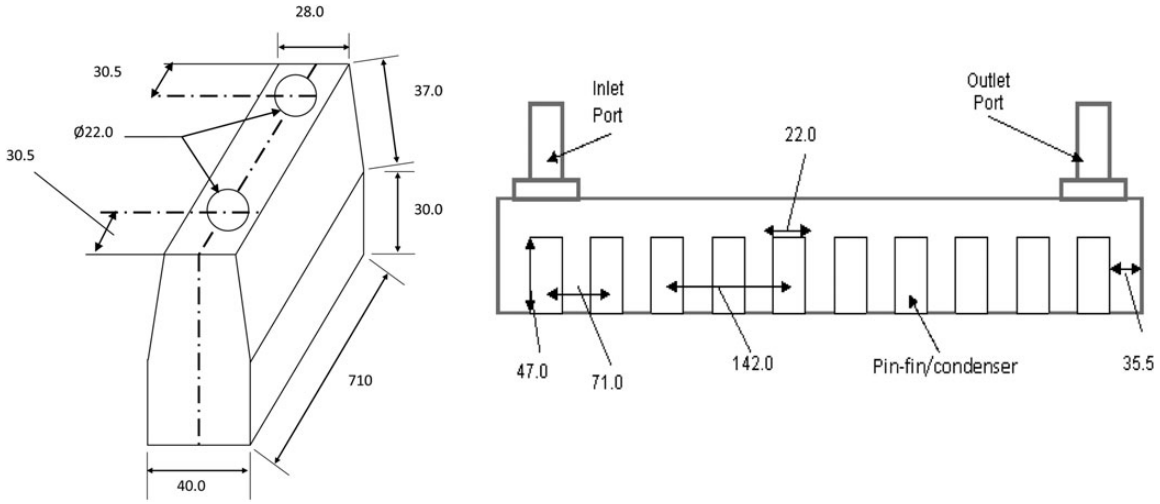

Figure 1. *3D cross-sectional and front views depicting the external and internal dimensions of model manifold chamber (not drawn to scale).*

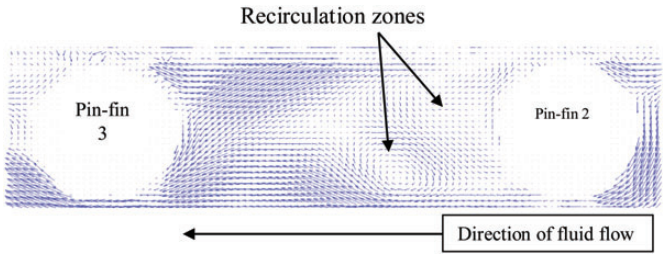

Figure 2. *Vector map 10 pin-fin configuration, fluid flow distribution observed in model manifold between* pin-fins 2 *and* 3, *mean velocity* $4 \times 10^{-3} m\ s^{-1}$.

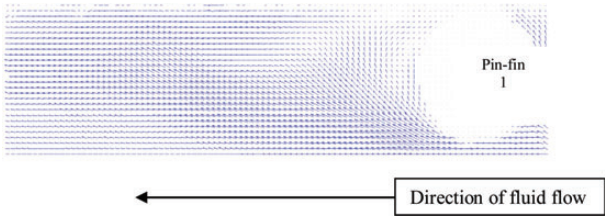

Figure 3. *Vector map 5 pin-fin configuration, fluid flow distribution observed in model manifold at* pin-fin 1, *mean velocity* $9 \times 10^{-3} ms^{-1}$.

fluid is constant, so flux conditions were similar to an operational solar water heater [21]. Two different pin-fin arrangements were investigated using the model manifold and both under simulated conditions of 1000 W m^{-2}; the 100-W cartridge heaters in the remaining five pin-fins were replaced by five 200-W cartridge heaters. The heaters were switched on in the manifold and left for 1 h to ensure that steady-state conditions were reached, seeding particles added and images of the manifold for each configuration collected so that visual comparisons could be made. Firstly, 10 pin-fins were used, simulating a conventional nonconcentrating heat-pipe evacuated tube manifold, then every other pin-fin was removed (1, 3, 5, 7, 9) and electrical energy supplied doubled. This kept the thermal input the same but reduced the area available for heat transfer by 50% to investigate the effect of using reflective concentrators on heat transfer and fluid flow. Each pin-fin had a t-type thermocouple ($\pm 0.1^{\circ}$C) located internally 3 mm from the surface of the pin-fin, Platinum-resistive thermometry devices (RTDs) were used to measure the temperature of the ambient, fluid entering and exiting the manifold to an accuracy of $\pm 0.1^{\circ}$C. Power was measured using voltage and current transducers to an accuracy of 1% and energy consumed measured using an electrical energy consumption meter to the nearest Wh.

3 RESULTS AND DISCUSSION

3.1 Image Processing

Fifty double-frame images of the fluid flow field around the manifold inlet were captured to determine if any observable differences between the two configurations could be visualized using 2D-PIV. For the 10 pin-fins configuration, images were collected from the area around *pin-fins 2* to *3*. For the five pin-fin configuration, images were collected from around *pin-fin 1*. Due to the layout of the model manifold, it was not possible to observe *pin-fin 1* in the 10 pin-fin configuration or *pin-fin 5* in the five pin-fin setup. A vector statistics map for each of the 50 processed vector maps was produced, image processing removes outlying and erroneous vectors [24].

3.2 Processed Images

The vector maps of the internal fluid flow regime of the entrance region under similar conditions derived from the image processing process are shown in Figures 2 and 3, for the 10 pin-fin (*pin-fins 2* and *3*) and 5 pin-fin model manifold configurations (*pin-fin 1*), respectively.

There are clear discernible differences between the two configurations; Figures 2 and 3 show the entrance region of the 10

pin-fin and 5 pin-fin configurations, respectively. Differences are observed with recirculation zones visible beside *pin-fin 2* in Figure 2 whereas these are absent and fluid velocity has increased by more than 100% in Figure 3. The Nusselt numbers for *pin-fins 2* and *3* in the 10 fin configuration were calculated as 124 and 218, respectively. For the five pin-fin configuration, the Nusselt number at *pin-fin 1* (located at same point as *pin-fin 2* in 10 pin-fin system) was calculated as 67; at the second pin-fin (*pin-fin 4* in 10 pin-fin configuration), it was 257. At the furthermost pin-fin in the 10 pin-fin array (pin-fin 10), the Nusselt number was 900; for the five pin-fin array, it was 1019. Over the measurement period, the 10 pin-fin model manifold had a heat removal efficiency 9% greater than the 5 pin-fin configuration but had twice the surface area available for heat transfer.

4 SIGNIFICANCE AND IMPACT OF RESULTS

Further application of this technique for investigating manifold design would lead to improved designs of thermosyphon heat-pipe ETSWHs reducing the cost to consumers while improving system reliability. The results have demonstrated that incorporating reflective concentrators and increasing the spacing between the pin-fins improves the fluid flow regime as fewer stagnant and recirculation regions are observed in Figures 2 and 3, and the Nusselt number across the model manifold increases to a higher maximum value of 1019 compared with 900 for the 10 pin-fin an 11.7% increase. This demonstrates that if effective 2× CPCs could be designed and incorporated then up to 50% of the evacuated tubes could be removed from the solar thermal collector substantially reducing the cost of production. By eliminating auxiliary power requirements for pumping, hot water can still be generated if power is lost. A recent report [25] on a field trial of solar water heaters operating in the UK reported that a typical system uses 55 kWh of electrical energy to circulate the heat transfer fluid. Maintenance and replacement of the pump (every 10 years) estimated as £90 by [1] would not be required if a collector life span of 25 years is assumed; so a saving of £270 at current costs over the operating life span of the system would be achieved. With typical installation costs currently being £4800 [1], having no parasitic power requirements and assuming that removal of 50% of the evacuated tubes reduces the cost by 30%, an installed cost of £3360 would be achievable. If this stimulated the market in ETSWH by 30% compared with sales in 2012, then the annual installed area would rise to 20 415 m^2 giving a capacity of 14 290 kW_{th}. Assuming each square meter of installed area can supply 500 kWh $year^{-1}$ [26], then annually 10 207 GWh of energy could be generated saving 4 082 920–66 34 745 kg CO_2 depending on whether the fuel substituted was natural gas or oil, respectively [27] kWh.

5 CONCLUSION

The construction of a model manifold that simulated the manifold of a heat-pipe ETSWH was described. 2D-PIV revealed significant differences in flow patterns between the two manifold configurations which were confirmed by comparing the Nusselt number at the same location. The five pin-fin configuration had a Nusselt number 2.1 times greater than that calculated at the same location in the 10 pin-fin configuration. The results indicate that the incorporation of concentrators would have a small effect on overall system efficiency but would reduce frictional losses internally. Substantial energy and carbon savings could be realized. Further work should be directed toward improving similar heat exchangers, so that efficiency can be maintained and reflective concentrators incorporated.

ACKNOWLEDGEMENT

The authors thank the technical support staff of the University of Ulster for their assistance with the experimental setup, technical advice, fabrication and machining skills. Without this, such work would not be possible. This paper was originally presented at the SOLARIS 2013 Conference.

REFERENCES

[1] Energy Saving Trust. *Solar Water Heating,* 29 December 2013. [Online]. http://www.energysavingtrust.org.uk/Generating-energy/Choosing-a-renewable-technology/Solar-water-heating#3 (29 December 2013, date last accessed).

[2] ESTIF, *Solar Thermal Markets in Europe Trends and Market Statistics 2012*, 1 June 2012. [Online]. http://www.estif.org/fileadmin/estif/content/market_data/downloads/Solar_Thermal_M%20arkets%202012.pdf (30 December 2013, date last accessed).

[3] DeVries H, Kamminga W, Francken J, Fluid cicrculation control in conventional and heat pipe planar solar collectors. *Solar Energy* 1980;**24**:209–213.

[4] Ortabasi U, Fehlner FP. Cusp mirror heat-pipe evacuated tubular solar thermal colector. *Solar Energy* 1980;**24**:477–489.

[5] Hull JR. Comparison of heat transfer in solar collectors with heat pipe versus flow through absorbers. *ASME J Solar Energy Eng* 1987;**109**:253–258.

[6] Norton B, Probert SD. Thermosyphon solar water heaters. *Adv Solar Energy* 1986;**3**:125–170.

[7] Winston R. Priniciles of solar concentrators of a novel design. *Solar Energy* 1974;**16**:89–95.

[8] O'Gallagher JJ. *Nonimaging Optics in Solar Energy.* Morgan and Claypool, 2008.

[9] Garcia-Valladares O, Pilatowsky I, Ruiz V. Outdoor test method to determine the thermal behaviour of solar domestic water heating. *Solar Energy* 2008;**82**:613–622.

[10] Anon., *Solar Heating-Domestic Water Heating Systems, Part 2: Outdoor Test Methods for System Performance Characterization and Yearly Performance Prediction Solar Only Systems, ISO 9459-2*. International Standard, Geneva, 1995.

[11] Budihardjo I, Morrison GL, Behnia M, Performance of a water-in-glass evacuated solar water heater. In: *Proceedings of Australian New Zealand Solar Energy Society, Newcastle, Australia*, 2002.

[12] Morrison GL, Budihardjo I, Behnia M. Water-in-glass evacuated tube solar water heaters. *Solar Energy* 2004;**76**:135–140.

[13] Budihardjo I, Morrison GL. Performance of water-in-glass evacuated tube solar water heaters. *Solar Energy* 2009;**83**:49–56.
[14] Lierberman J, Gebhart B. Interactions in natural convection from an array of heated elements, experimental. *Int J Heat Mass Transfer* 1969;**12**: 1385–1389.
[15] Corcione M. Interactive free convection from a pair of vertical tube-arrays at moderate Rayleigh numbers. *Int J Heat Mass Transfer* 2007;**50**: 1061–1074.
[16] Morgan VT. The overall convective heat transfer from smooth circular cylinders. *Adv Heat Transfer* 1975;**11**:119–264.
[17] Farouk B, Guceri SI. Natural convection in interacting flow fields. *Int J Heat Mass Transfer* 1983;**26**:231–243.
[18] Corcione M, Correlating equations for free convection heat transfer from horizontal isothermal cylinders set in a vertical array. *Int J Heat Mass Transfer* 2005;**48**:3660–3673.
[19] Morrison GL, Budihardjo I, Behnia M. Measurement and simulation of flow rate in a water-in-glass evacuated tube solar water heater. *Solar Energy* 2005;**78**:257–267.
[20] Morrison GL, Ranatunga DBJ. Thermosyphon circulation in solar collectors. *Solar Energy* 1980;**24**:191–198.
[21] Redpath DAG, Eames PC, Lo SNG, Griffiths PW. Experimental investigation of natural convection heat exchange within a physical model of the manifold chamber of a thermosyphon heat-pipe evacuated tube solar water heater. *Solar Energy* 2009;**83**:988–997.
[22] Redpath DAG. Thermosyphon heat-pipe evacuated tube solar water heaters for northern maritime climates. *Solar Energy* 2012;**86**:705–715.
[23] Redpath DAG, Griffiths PW, Lo SNG, Herron MG. Experimental investigation of fluid flow regime in thermosyphon heat-pipe evacuated tube solar water heaters. in *PLEA, Towards Zero Energy Buildings*, Dublin, 2008.
[24] Anon., *Dynamic Studio v3.14 User's Guide*. Dantec Dynamics. Skovlunde, 2010.
[25] Energy Saving Trust. *Here Comes the Sun: A Field Trial of Solar Water Heating Systems*, 30 September 2011. [Online]. http://www.energysavingtrust.org.uk/Publications2/Generating-energy/Field-trial-reports/Here-comes-the-sun-a-field-trial-of-solar-water-heating-systems (31 December 2013, date last accessed).
[26] DGS, *Planning and Installing Solar Thermal Systems: a Guide for Installers, Architects*, the German Solar Energy Society. James and James, 2005.
[27] I. E. Agency. *CO_2 Emissions From Fuel Combustion Highlights 2012*, 31 October 2012. [Online]. http://www.iea.org/co2highlights/co2highlights.pdf (31 December 2013, date last accessed).